Synthesis and Spectral Properties of Gem-Dimethyl Chlorin Photosensitizers

Preprint · March 2020

DOI: 10.26434/chemrxiv.12017118

5 authors, including:

Zoi Melissari
Trinity College Dublin
8 PUBLICATIONS **11** CITATIONS
SEE PROFILE

Harry Charles Sample
6 PUBLICATIONS **32** CITATIONS
SEE PROFILE

René M Williams
University of Amsterdam
119 PUBLICATIONS **4,352** CITATIONS
SEE PROFILE

Mathias O. Senge
Trinity College Dublin
605 PUBLICATIONS **13,510** CITATIONS
SEE PROFILE

Synthesis and spectral properties of *gem*-dimethyl chlorin photosensitizers

Zoi Melissari,[a,b] Harry C. Sample,[a] Brendan Twamley,[c] René M. Williams*[b] and Mathias O. Senge*[a]

Abstract: Chlorins that bear a *gem*-dimethyl group, which attributes their resistance to oxidation, are of interest for applications in photomedicine. Herein, we present the synthesis and the photophysical properties of two *geminal*-dimethyl chlorins (dihydroporphyrins) and their free base counterparts that act as efficient singlet oxygen generators and thus exhibit potential for use in photodynamic therapy (PDT) as anticancer or antimicrobial agents upon further derivatization. A complete characterization of their spectral and photophysical properties (Φ_f, Φ_{isc}, Φ_{ic}, Φ_Δ, τ_S, τ_T, k_f, k_{ic}, k_{isc}, k_q) is accompanied by density functional calculations (DFT) as well as time dependent (TD) DFT to investigate the features of the frontier molecular orbitals. To demonstrate the potential of these compounds, standard palladium mediated reaction yielded a porphyrin-chlorin dyad in moderate yield.

Introduction

Photodynamic therapy (PDT) is a non-invasive therapy which involves systemic or topical administration of a photosensitizer (PS), light, and molecular oxygen. Under the effect of light, molecular oxygen can generate highly reactive singlet oxygen ($^1O_2$) along with other reactive oxygen species (ROS) which can lead to specific apoptotic or necrotic cell death of cancer cells (Figure 1). An ideal PS should specifically accumulate in the target tissue, have low dark toxicity, high phototoxicity, quick clearance from the body and, have a strong absorption in the red or near-infrared region of the electromagnetic spectrum (600 – 800 nm). The latter enables light to penetrate deep into the target tissue and activate the PS. Most of the PSs that are synthesized and investigated for PDT treatment are based on tetrapyrrolic structures. Thus, porphyrins,[1] chlorins,[2] bacteriochlorins,[3] or phthalocyanines,[4] are potential candidates.

Chlorins are envisaged as diagnostic and therapeutic agents and have found use in materials chemistry applications.[5] They differ from porphyrins in having one reduced pyrrole ring which does not reduce the π-conjugation of the macrocycle, but results in a vast difference in the UV-Visible spectrum through the change of the symmetry of the macrocycle allowing for longer wavelength transitions.[6] An efficient PS can be developed by modifying the core structure and modulating their photophysical properties. The desirable photophysical characteristics include a high quantum yield of triplet formation ($\Phi_T \geq 0.5$), a large singlet oxygen quantum yield ($\Phi_\Delta \geq 0.5$), relatively long triplet state lifetime (τ_T, in the µs range), and a high triplet state energy (≥ 94.3 kJ mol^{-1}).

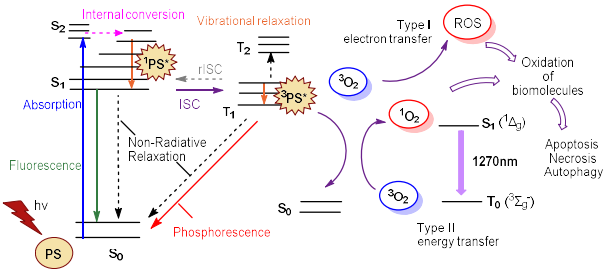

Figure 1. Simplified Jablonski diagram showing the pathways after photoactivation of a PS.

Chlorins are highly conjugated systems and have a characteristic UV-Vis spectrum with strong absorption between 600 – 800 nm with a high extinction coefficient. Absorption at such a long wavelength allows for deeper penetration of tissues, and more successful treatment with PDT. The strong absorption in the range of 400 – 800 nm (400 – 450 nm: Soret or B band and 500 – 800 nm: Q bands) is caused by the splitting of the frontier molecular orbitals (FMOs), well described with Gouterman's four orbital model (HOMO-1, HOMO, LUMO, and LUMO+1 orbitals) for the chlorin macrocycle.[7] Reducing the HOMO – LUMO gap by destabilizing the specific MOs can lead to the red-shifted absorption profile that it is of major importance in PDT. Also, the identity of a central metal ion and the substituents influence the relative energies of the MO transitions. The Soret band stems from the strong electronic transition from the ground state to the second excited singlet state $S_0 \rightarrow S_2$ and the Q bands from the transition to the first excited singlet state $S_0 \rightarrow S_1$. The loss of energy by internal conversion (IC) is very fast that the fluorescence is observed from the depopulation of the first excited singlet state to the ground state $S_1 \rightarrow S_0$. The fluorescence quantum yield needs to be moderately high for use in diagnostics and imaging.[8,9] However, for PDT, it is the triplet state quantum yield that is more important as well as enhancing the intersystem crossing (ISC) $S_1 \rightarrow T_1$ (Figure 1). This can be achieved by introducing heavy atoms like transition metals or halogens (heavy atom effect).[10,11] Moreover, the triplet excited state lifetime should be sufficiently long-lived, and the triplet energy state should be higher than that of the singlet oxygen, so it can efficiently produce moderate yields of the later through energy transfer (Type II).

Chlorins normally satisfy the above criteria even in the absence of transition metal ions or halogens.[8] The photophysical properties of chlorins are solvent dependent and, in some cases, charge transfer (CT) can happen and access the desired triplet state *via* ISC.[12,13] The singlet oxygen lifetime in

[a] Prof. Dr. Mathias O. Senge, Harry C. Sample, Zoi Melissari
Medicinal Chemistry, Trinity Translational Medicine Institute, Trinity Centre for Health Sciences, Trinity College Dublin, The University of Dublin, St James's Hospital, Dublin 8 (Ireland)
E-mail: sengem@tcd.ie; twitter: @mathiassenge
http://chemistry.tcd.ie/staff/people/mos/Home.html:
[b] Dr. René M. Williams, Zoi Melissari
Van 't Hoff Institute for Molecular Sciences, University of Amsterdam, P.O. Box 94157, 1090 GD Amsterdam (The Netherlands)
[c] Dr. Brendan Twamley
School of Chemistry, Trinity College Dublin, The University of Dublin, College Green, Dublin 2 (Ireland)
Supporting information for this article is given via a link at the end of the document.

different solvents has been determined to be in the µs scale from time-resolved phosphorescence experiments by Ogilby and co-workers.[14] However, singlet oxygen has shorter lifetimes in biological media (~10 – 320 ns in cells) and it can only react with biomolecules in its proximity (10 – 55 nm). Thus, efficient PS should also have a high triplet yield and thus long-lived triplet state lifetime that can induce cell death *via* apoptosis, necrosis, and autophagic cell death.[15,16]

As for chlorin-based drugs benzoporphyrin derivative monoacid ring A (BPD-MA, Verteporfin) is used in the treatment of age-related macular degeneration (AMRD),[17] but not used for anti-cancer PDT due to its pharmacokinetic profile.[18] Chlorin-e_6 is a compound that has received remarkable attention over recent years for its use in PDT with a wide variety of derivatives being synthesized.[19,20] 5,10,15,20-Tetrakis(3-hydroxyphenyl)chlorin (*m*-THPC, Temoporfin, Foscan), is a synthetic chlorin which is currently used in the treatment of squamous cell carcinoma of the head and neck.[21,22] Given the possibility of oxidation of two of the aforementioned chlorins to porphyrins (*m*-THPC and chlorin-e_6), and the lack of further functionalization in the others (BPD-MA and *m*-THPC), there is significant room for improvement. We envisage 17,18-dihydro-18,18-dimethylporphyrins as solutions to these shortcomings.

Herein we present the synthesis; characterization and photophysical evaluation of two *gem*-dimethyl metallochlorins with meso-substituents, **Zn1** and **Zn2**, and their free base counterparts, **$H_2$1** and **$H_2$2**. These chlorins bear a *gem*-dimethyl group in the reduced pyrrole ring that prevents oxidation and thus ascribes stability advantages to the chlorins. Numerous similar complexes have been synthesized; however, little advances have been made to investigate their potential of singlet oxygen generation and to introduce such systems as PSs for application in PDT. This class of molecules, to our knowledge, has not been evaluated for PDT. They have however been localized in cells to understand the generation of $^1O_2$ inside cells.[23] We have studied these molecules by using steady state and time resolved spectroscopy to define their suitability as potential PSs through their singlet oxygen generation (through its luminescence emission at 1275 nm) and their singlet and triplet states lifetimes. We discuss their suitability as building blocks for PSs in PDT and present photophysical and single crystal X-ray diffraction studies.

Results and Discussion

Synthesis

The synthesis of *gem*-dialkyl chlorins can be performed through two separate methods: 1) rearrangement of a dialkyl pyrrolic unit to the *gem*-dialkyl under acidic conditions or 2) introduction of the *gem*-dialkyl group in one of the pyrrolic units and subsequent condensation. The flexibility present in the syntheses of the chlorins of today stems from the far-reaching and groundbreaking studies of the Lindsey group.[24] Comprising of a tetrahydrodipyrrin and a brominated-formylated-dipyrromethane, the Lindsey [2+2]-type synthesis is the most suitable way to synthesize these molecules on realistic scales. The two step one-pot reaction consists of an acid catalyzed pyrrole-aldehyde condensation, thus forming the linkage between the *A* and *B* rings, yielding the non-isolated 2,3,4,5-tetrahydrobiladiene-*ab*. This is then subjected to basic conditions, metallation and an oxidant.

With this in mind, we targeted two chlorins, bearing different aryl groups on the 10-position, utilizing this synthesis. The 4-bromophenyl was introduced to enhance the ISC and allow further functionalization through Pd-catalyzed cross-coupling reactions, and the 1-naphthyl substituent was introduced in order to understand the differing photophysical properties introduced by the 10-substitutent.

Western Half – 2,3,4,5-tetrahydro-1,3,3-trimethyldipyrrin (7). Initially targeting an unsubstituted variant of Battersby's western half,[25] Lindsey and co-workers found 2,3-dihydro-1,3,3-trimethyldipyrrin to be unstable, and subsequent condensation yields were low.[26] Modification of cyclization conditions yielded the respective tetrahydro derivative which is used unanimously today.[27] Labelled 'a deceptively simple precursor',[28] there have been multiple attempts at refining the synthesis of 2,3,4,5-tetrahydro-1,3,3-trimethyldipyrrin (**7**) and thus, we have been able to select certain syntheses in order to obtain the highest yield of this valuable intermediate. All syntheses start from pyrrole-2-carboxaldehyde and follow the sequence: Henry addition, reduction, Michael addition and, reductive cyclization (Scheme 1).

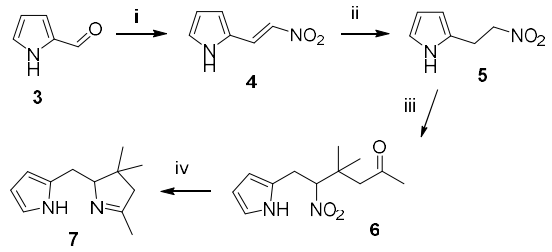

Scheme 1. Optimized synthesis of **7** from pyrrole-2-carboxaldehyde (**3**) over four steps in 30% yield. i) $MeNH_2{\cdot}HCl$, KOAc, $MeNO_2$, EtOH, rt, 2 h. ii) $LiBH_4$, THF, -10 °C, 0.25 h. iii) mesityl oxide, DBU, rt, 24 h. iv) $Zn/HCOONH_4$, THF, 40 °C, 26 h.

Henry addition of nitromethane to **3** in EtOH generated **4** in excellent yield,[29] and subsequent reduction with $LiBH_4$ yielded the nitro-ethyl intermediate, **5**, in good yield.[30] Although the use of $LiBH_4$ was introduced as a method to keep pyrrolic esters intact, we have found it to be more suitable than $NaBH_4$ over the same step. Michael addition of mesityl oxide in neat DBU afforded nitrohexanone **6** in good yield, and subsequent cyclization with $Zn/HCOONH_4$ yielded the desired dipyrrin in 48% yield, and thus **7** in 30% over four steps. Compounds **3**, **4**, and **5** could be purified simply by elution through silica plugs as opposed to column chromatography, thus reducing the amount of time spent in contact with SiO_2; however, compounds **6** and **7** still require column chromatography.

Eastern Half – 9-Bromo-1-formyl-5-substituted dipyrromethanes (10a,b). The synthesis of 5-substitued DPMs has been improved and continually refined during the last three decades by the Lindsey group through the reduction of oligomer production (by-products) in a one-flask synthesis, optimizing the acidic condensation, and purification methods.[30] Hence, synthesis of the eastern half of these chlorins (derivatives of 9-bromo-1-formyl-dipyrromethanes (DPMs)) were synthesized according to literature procedures (Scheme 2).

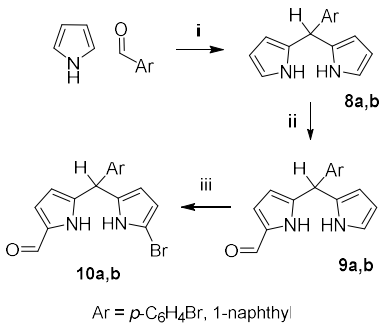

Scheme 2. Synthesis of 9-bromo-1-formyl-dipyrromethanes **10a** and **10b** over three steps. i) TFA, rt, 1 – 1.5 h. ii) DMF/$POCl_3$, 0 °C, 2 h, EtOAc/NaOAc. iii) NBS, THF, -78 °C, 1 h.

For **8a-b**, Cl_2CH_2 was used together with pyrrole as the solvent and hence reducing the concentration of pyrrole. Thus, using 10 eq. of pyrrole and 0.1 eq. of trifluoroacetic acid (TFA), we obtained **8a** in 48% yield and **8b** in a yield of 56%. Subsequent Vilsmeier-Haack formylation of the DPMs utilizing $POCl_3$/DMF yielded **9a** and **9b** in 39% and 42% yields,[31] respectively. The diformylated products were observed by TLC; however, these were not isolated or characterized. Lastly, electrophilic aromatic substitution using 1 eq. of NBS in anhydrous THF yielded the desired 9-bromo-1-formyl-dipyrromethanes **10a** and **10b** in 70% and 55% yields respectively.[32] In some cases, bromination of 1-formyl-DPMs yielded multiple products, and likewise these were not isolated.

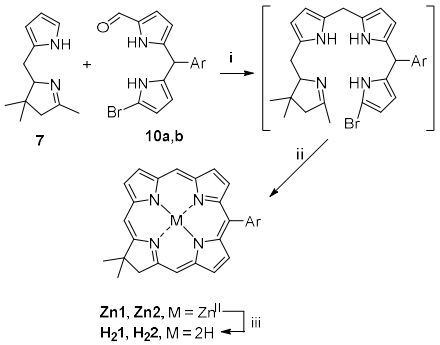

Scheme 3. Synthesis of *gem*-dimethyl chlorins from **7** and either **10a** or **10b**, displaying the non-isolated 2,3,4,5-tetrahydrobiladiene-*ab*, and the final metallochlorin product. i) *p*-TsOH·H_2O, CH_2Cl_2/CH_3OH, 20 °C, 0.5 h. ii) 2,2,6,6-tetramethylpiperidine, $Zn(OAc)_2$, AgOTf, 90 °C, 18 – 20 h, CH_3CN. iii) TFA/CH_2Cl_2, 20 °C.

17,18-Dihydro-18,18-dimethylporphyrins. Syntheses of the targeted chlorins bearing a *gem*-dimethyl group was performed using synthesis reported by Ptaszek *et al*. (Route II).[33] Thus, **7** was reacted with **10a** or **10b** and 5 eq. of *p*-TsOH•H_2O in CH_2Cl_2/CH_3OH for 30 min and the subsequent removal of the solvent resulted in the yielding of the non-isolated intermediate, tetrahydrobiladiene-*ab*. This was immediately treated with CH_3CN, 2,2,6,6-tetramethylpiperidine, anhydrous $Zn(OAc)_2$, AgOTf and was allowed to stir at 90 °C for 18 – 20 h. The products formed were either the desired chlorin or degraded products (which are baseline on TLC). Therefore, the desired chlorin products were isolated after column chromatography as blue-purple solids in good yields (37% for **Zn1** and 36% for **Zn2**). Demetallation of **Zn1** and **Zn2** were carried out by using TFA in CH_2Cl_2 to yield the free-base counterparts as green solids (46% for **$H_2$1** and 41% for **$H_2$2**).

During the preparation of this manuscript, we became aware of the recent publication of Borbas *et al*.,[34] and some differences can be drawn between our syntheses; 1) isolation of the final brominated-formylated-dipyrromethane has a drastic effect on the final yield of the chlorin: the yield of **Zn1** isolated by Borbas was 21%, under half we report, and 2) the demetallation of the chlorins can be done faster with a lower concentration of TFA, and quenching with NEt_3 is far more fruitful than the use of $NaHCO_3$ presented herein.

These compounds were characterized, regarding their ground and excited photophysical properties and their singlet oxygen generation. Additionally, compounds **Zn1** and **$H_2$1** were further characterized by single-crystal X-ray diffraction analysis and crystal structures obtained (see below).

Porphyrin-chlorin dyad (12). The chlorin core can be modified *via* several approaches with the most common one being bromination and subsequent palladium-catalyzed cross coupling reactions. Bromination can be achieved either from constructing the bromo-chlorin (preparation of the bromo-substituted Eastern and Western halves) or subjecting the intact chlorin to direct bromination.[35] Then, palladium-catalyzed cross-coupling reactions such as Suzuki,[36] or Sonogashira,[37,38] can introduce the desired substituents in the chlorin periphery. Herein, the meso-borylated porphyrin (**11**)[39] reacted smoothly under standard Suzuki cross-coupling conditions to yield the porphyrin-chlorin dyad (**12**) (Scheme 4). The chlorin and porphyrin macrocycles are connected *via* the meso-position through a phenylene linker. It is previously reported that such structures can enhance electron transfer processes. Additionally, through two photon absorption this type of compound gives rise to new applications and prospects in the field of bioimaging and PDT.[40]

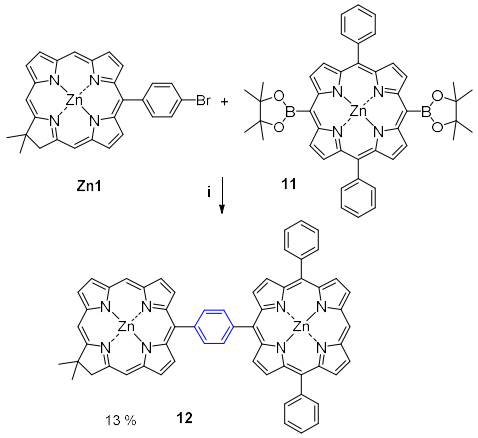

Scheme 4. Suzuki cross coupling reaction between compound **Zn1** and **11**. i) 10 eq. Cs_2CO_3, 0.2 eq. $Pd(PPh_3)_4$, toluene/DMF, 2:1, 3 h, 85 °C.

Spectroscopic Studies

The chlorins synthesized herein were investigated with regard to their ground and excited state properties, and together with the singlet oxygen generation, we illustrate that they possess desirable photophysical and -chemical characteristics suitable for use as PSs. We have experimentally determined the yields and rate constants of the decay pathways of the singlet excited state (S_1) and estimated the triplet energy state for each chlorin

(T_1) through the use of DFT (Density Functional Theory) calculations.

Ground state properties. Normalized UV-Visible absorption spectra of all compounds are displayed in Figure 2. The free-base and Zn(II) chlorins display absorption spectra that differ greatly from each other due to the metal effect.

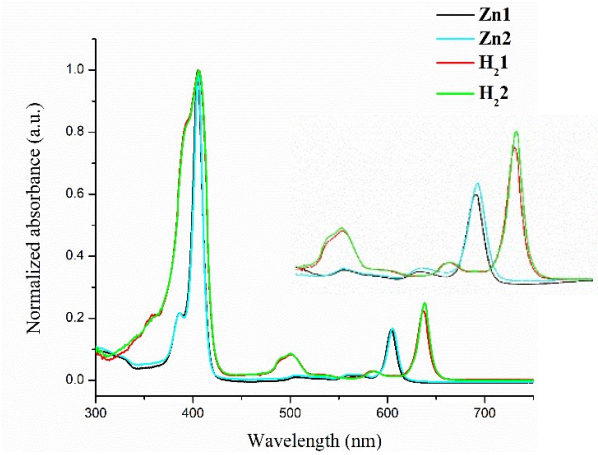

Figure 2. UV-Vis absorption spectra of the chlorins in ethanol (**Zn1**, **Zn2**) and free-base chlorins in dichloromethane (**H₂1**, **H₂2**). Spectra are normalized at the maximum of the B bands (inset shows Q-bands).

The absorption spectra of chlorins show a strong B-band in blue-violet region ~400 nm, with minor difference between Zn(II) chlorins and their free base analogues. The last Q-band of the free base chlorins exhibits a significant red shift (ca. 30 nm) as compared to Zn(II) complexes, which is probably due to reduction in HOMO-LUMO gap. Coordination with Zn(II), that acts as a Lewis acid by accepting electron density from the macrocycle, results in stabilization of the chlorin core and thus lowers the energies of the MOs.[41] Furthermore, the ratio of the intensity of the $Q_y(0,0)$ and B bands (see Table S1) provides a relative measure of the hyperchromic effect on the $Q_y(0,0)$ band showing the following descending order **H₂2** > **H₂1** > **Zn2** > **Zn1**. Comparison of these compounds by means of the meso-substituents indicates there is no dramatic difference between the 4-bromophenyl and 1-naphthyl group; only a slight bathochromic shift for the Q_y band, in favor of the naphthalene substituent. A broader Q_x band for **H₂1** and **H₂2** is displayed at ~500 nm, which is indicative of different electronic transitions occurring, in comparison with **Zn1** and **Zn2**, due to the vibronic borrowing from the strong B transitions.[17,42]

Singlet and triplet excited state properties. Fluorescence quantum yields and lifetimes in ethanol and methanol, together with the radiative and non-radiative rates, are shown in Table 1. Fluorescence emission is detected by the $S_1 \rightarrow S_0$ transition as the IC from $S_2/S_n \rightarrow S_1$ is very fast and undetectable. Fluorescence spectra of the chlorins are dominated by the $Q_y(0,0)$ band of the absorption spectrum with a shoulder at the $Q_y(1,0)$ band, the vibronic satellite. Compounds **Zn1** and **Zn2** display a fluorescence peak maxima (λ_{max}) at ca. 610 nm with a vibronic satellite, at ~660 nm while compounds **H₂1** and **H₂2** display their peak maxima at ca. 638 nm with two vibronic satellites at 667 and 700 nm (Figure 3). A minor Stokes shift from 50 to 160 cm^{-1} (2 to 6 nm) occurs between $Q_y(0,0)$ absorption and Q_y emission peak with the free base chlorins displaying a smaller shift (50 – 70 cm^{-1}).

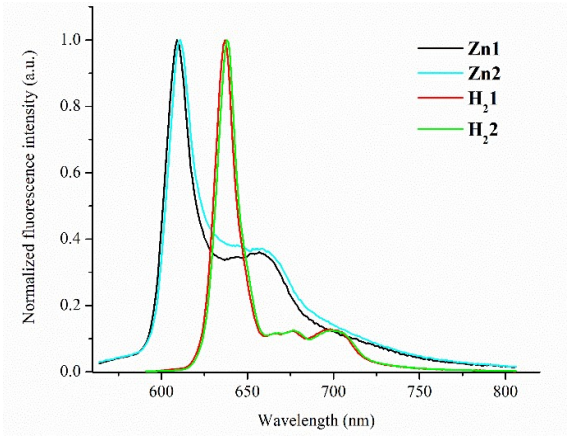

Figure 3. Normalized fluorescence emission spectra of the chlorins in ethanol.

Fluorescence quantum yields (Φ_f) of **Zn1** and **Zn2** range from 0.03 to 0.08, respectively and from 0.08 to 0.14 for **H₂1** and **H₂2**, respectively. The Φ_f of the free base chlorins is around two times higher than the Φ_f of the Zn(II) chelates. Furthermore, as expected, the fluorescence lifetime of **Zn1** and **Zn2** is between 1 – 1.5 ns whilst that of **H₂1** and **H₂2** is between 5 – 7 ns. Thus, Zn(II) derivatives have an almost five times shorter fluorescence lifetime as compared to the free base, which indicates that Zn(II) chelates undergo faster ISC to the triplet excited state in comparison to the free base counterparts due to the heavy atom effect.[17][1,] Additionally, the lowest Φ_f is displayed by chlorins **Zn1** and **H₂1** with the 4-bromo-phenyl substituent. The results are comparable with the literature of similar compounds.[42b,43]

Time-correlated single photon counting (TCSPC) was performed and the fluorescence decay profiles of each chlorin in ethanol and methanol are shown in Figures S27 – S34. Lifetime values of the singlet excited state (τ_S) remains the same between ethanol and methanol solutions for all the chlorins. The radiative ($k_r = k_f$ = fluorescence rate constant) and non-radiative ($k_{nr} = k_{ic} + k_{isc}$) rate constants, were calculated by using equations 1 and 2, following reported methods and are summarized in Table 1.[44,45]

$$k_x = \Phi_x \div \tau_{S,} \qquad (1)$$

where x is *f*, ISC or IC.

$$\Phi_{IC} = 1 - \Phi_{ISC} - \Phi_f \qquad (2)$$

As ISC possesses a dominant role in the photochemical pathway for the chlorins, nanosecond transient absorption (TA) spectroscopy was performed and the triplet state quantum yields (Φ_T or Φ_{ISC}) were calculated from the triplet-triplet absorption spectra, and these can be seen in Figures S10 – S17 and S19 – S26. Triplet state lifetimes (τ_T) at ambient and oxygen-free conditions (through degassing with argon) in methanol or ethanol are shown in Table 1. Stimulated emission spectra which appeared at early delay times were not taken into consideration for the triplet lifetime calculation. Nevertheless, these features allowed us to estimate the triplet state quantum yield as they contain the singlet state features. Consequently, the IC quantum yield (equation 2) along with the corresponding rate constants (k_{ic}, k_{isc}) were calculated and are also presented in Table 1.

It is indicated that the shorter fluorescence lifetime of the Zn(II) chlorins compared to the free base counterparts is due to the heavy atom effect. Triplet state yields are higher in the zinc chelates (Φ_T ~ 0.75 – 0.94) with a descending order **Zn1** > **Zn2** > **$H_2$1** > **$H_2$2** showing the more dominant pathway of IC and ISC (k_{nr}). The k_f values of **Zn1** and **Zn2** are typical for Zn(II) chlorins as are the k_{nr} values of the free base analogues.[42b]

The triplet absorption profile of the TA spectra of metallochlorins (**Zn1**, **Zn2**) and the free base chlorins (**$H_2$1**, **$H_2$2**) display very similar shapes, both in ethanol and methanol. Figure 4 displays representative TA spectra of one Zn(II) chlorin (**Zn1**; top) and the free base counterpart (**$H_2$1**; bottom). They show an absorption maximum at 420 – 460 nm and negative absorbance signals that are caused by bleaching of the ground-state, which is characteristic of the significant electronic transitions at 400 – 500 nm (B band) and 600 – 650 nm (Q_y band). The lifetime of the Zn(II) chelates under ambient conditions is longer than that of the free base chlorins. In contrast, the Zn(II) complexes display shorter lifetimes in oxygen free conditions, which shows that free base compounds have intrinsically longer triplet lifetimes. There is a large difference from the ns to the μs time scale at ambient and in oxygen free conditions. This indicates that oxygen plays a significant role in chemical processes upon photoirradiation and, energy transfer from the triplet state of the molecules to molecular oxygen in the microenvironment takes place efficiently. Indeed, the singlet oxygen quantum yield is relatively high for both **Zn1** and **Zn2** in methanol and ethanol, and in the latter, it reaches 90 % while **$H_2$1** and **$H_2$2** show lower singlet oxygen quantum yields as expected due to their lifetimes and rates. The Stern–Volmer equation was applied to calculate the energy transfer of the compounds from the triplet state to molecular oxygen (k_q) (equation 3),[46]

$$k_q = [(1/\tau) - (1/\tau^0)] \div [O_2] \qquad (3)$$

where; k_q is the rate constant for quenching of the triplet state by oxygen, τ^0 the triplet lifetime in oxygen free conditions, τ the triplet lifetime in the presence of oxygen and, $[O_2]$ is the concentration of oxygen which is in methanol and ethanol at 20 °C $[O_2] = 2.1 \times 10^{-3}$ M.[47] Values are shown in Table 1 and they are consistent with other chlorin molecules in the literature.[48,49]

Table 1. Photophysical properties of the chlorins.

Chlorin	λ_{em} (nm)	Stokes shift [a] (cm^{-1})	τ_s (ns)	τ_T [b] (ns)	τ_T [c] (μs)	Φ_f	Φ_{isc}	Φ_{ic}	Φ_Δ	k_f ×10^7 s^{-1}	k_{isc} ×10^8 s^{-1}	k_{ic} ×10^7 s^{-1}	k_q [d] (× 10^9 M^{-1} s^{-1})
Zn1[*]	609	163	0.9	200	27	0.03	0.80	0.17	0.58	3.3	8.9	19	2.36
Zn1[**]	609	136	0.9	202	26	0.04	0.94	0.02	0.90	4.4	10	2.2	2.34
Zn2[*]	611	162	1.5	210	28	0.05	0.78	0.17	0.55	3.3	5.2	11	2.25
Zn2[**]	611	162	1.5	210	30	0.08	0.88	0.03	0.85	5.3	5.9	2.0	2.25
$H_2$1[*]	637	74	5	160	47	0.07	0.78	0.15	0.40	1.4	1.6	3.0	2.97
$H_2$1[**]	637	74	5	170	70	0.08	0.80	0.12	0.70	1.6	1.6	2.4	2.79
$H_2$2[*]	637	50	7	150	50	0.10	0.70	0.20	0.38	1.4	1.0	2.9	3.17
$H_2$2[**]	638	50	7	166	64	0.14	0.75	0.11	0.60	2.0	1.1	1.6	2.86

[a] The Stokes shift was calculated from the corresponding UV-Vis and emission spectra in EtOH or MeOH; [b] triplet state lifetime in air (equilibrated); [c] triplet state lifetime in oxygen free solution; [d] oxygen quenching rate; [*] MeOH; [**] EtOH; typical errors (percentage of value) are τ_s ±5%, τ_T ±10%, Φ_f ±10%, Φ_{isc} ±10 %, Φ_{ic} ±15%, Φ_Δ ±10%, k_f ±10%, k_{ic} ±10%, k_{isc} ±10%, k_q ±15 %.

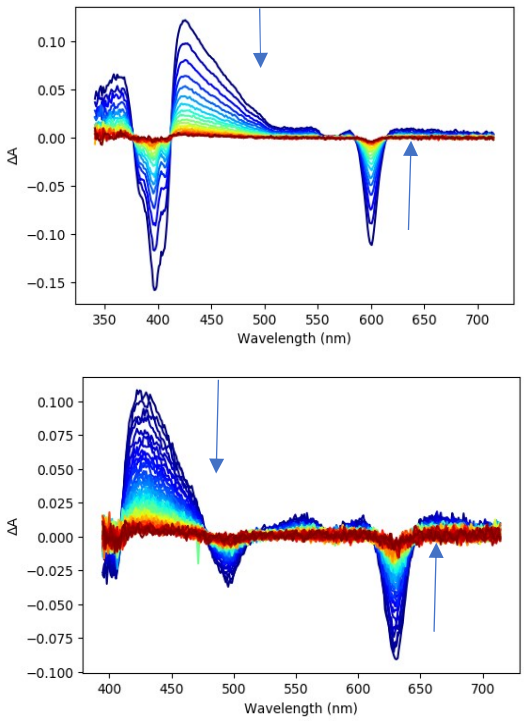

Figure 4. TA spectra of **Zn1** in methanol (ambient conditions; 0.5 absorbance value at 604 nm; incremental time 40 ns; 604 nm λ_{exc}) on the top; TA spectra of **$H_2$1** in methanol (oxygen free conditions; 0.5 absorbance value at 637 nm; incremental time 3000 ns; 637 nm λ_{exc}) on the bottom. Arrows from blue to red color show the decay from the maximum intensity in the successive steps respectively.

Initial results from transient absorption spectroscopy showed that **12** has a moderate triplet lifetime (190 ± 20 ns, Figure S18) and low fluorescence yield in methanol (0.02, Figure S9). Further photophysical experiments are ongoing to elucidate the chemical processes after photoirradiation.

Singlet oxygen quantum yield (Φ_Δ). Direct detection of the luminescence emission of singlet oxygen at 1275 nm was achieved using a InGaAs detector, cooled with liquid nitrogen. Singlet oxygen quantum yield (Φ_Δ) determinations in polar solvents were performed and the values are shown in Table 1.

As previously mentioned, when chlorins undergo ISC as the dominant decay pathway ($S_1 \rightarrow T_1$), this triplet excited state reacts with molecular oxygen and produces singlet oxygen ($^1O_2$). The triplet energy of an ideal PS should be higher than the lowest excited singlet state of molecular oxygen (94.3 kJ.mol^{-1} or 0.977 eV) to be able to generate singlet oxygen. It is reported that in chlorinated solvents such as CH_2Cl_2,[50] the singlet oxygen quantum yield can be overestimated; thus, ethanol and methanol were used with regards to their future compatibility for in vitro evaluation.

All the chlorins exhibit high Φ_Δ both in methanol and ethanol, however ethanol appears to have a greater effect on the singlet oxygen generation than methanol. Singlet oxygen lifetime depends on the solvent's reactivity (15 µs in ethanol; 9 µs in methanol) and given that the triplet state lifetimes of the chlorins, and that the [O_2] does not differ between the two solvents, this can attribute to the Φ_Δ difference between methanol and ethanol reported in this work.[51] Additionally, as the luminescence of singlet oxygen is very sensitive to detection, longer time integrals were used for the Φ_Δ measurements. As a result of the short fluorescence lifetimes, high ISC quantum yields, and longer triplet state lifetimes, **Zn1** and **Zn2** display higher values on average in both solvents (0.55 – 0.90) when compared with the free base counterparts (0.40 – 0.70) while **Zn1** and **$H_2$1** display slightly higher values, as a result of the 4-bromophenyl substituent (Figures S35 – S38).

DFT and TDDFT calculations. Density functional theory (DFT) and time-dependent DFT (TDDFT) calculations were performed to investigate the ground-state and the excited-state properties of the chlorins. DFT calculations were performed in gas phase with the hybrid B3LYP functional and a 6-31G* basis set to optimize the ground singlet state (S_0) geometry of the molecules. Then, with the optimized ground state geometry, TDDFT was performed to calculate the excited singlet state (S_1) and the respective molecular orbitals (MOs). Our goal was to determine the theoretical singlet and triplet excited level of the chlorins, compute the singlet-triplet gap and visualize the electron-density distribution in HOMOs and LUMOs (Figure 5). The energy levels (eV) and the S_1 ($^1E_{00}$) and T_1 ($^3E_{00}$) energies are shown in Table 2 along with the energy difference between [HOMO-LUMO], [(HOMO-1) – LUMO] and [(HOMO-1) – (LUMO+1)].

In all the optimized structures, the HOMO-1 shows the electron density localized on the four meso-positions. In the free base chlorins, it is also localized on the core N-atoms, whereas, in the Zn(II) analogues it is also localized on the core metal atom. In accordance to a previous report by Aravindu and coworkers,[42b] HOMOs do not show electron density at meso-positions; hence, the substitution at meso-position/s can significantly alter the HOMO-1 energy level that is visible in the UV-Vis spectra of the complexes. The same group applied the four-orbital model to assign the electronic transitions from the calculations to the experimental spectra. This proved that the HOMO-1 → LUMO and HOMO → LUMO+1 correspond to B_x and Q_x bands and HOMO-1 → LUMO+1 and HOMO → LUMO correspond to Q_y bands. This can be applied to the corresponding chlorins, as they have similar properties, energies, and electron-density of MOs.[42b,52] The corresponding unrestricted open-shell (UB3LYP) DFT method and 6-31G* basis set were used to calculate the triplet excited state T_1 following the theoretical method of Brückner *et al.*,[53] The difference between the first singlet excited and triplet energy state ($\Delta E_{S\text{-}T}$) and triplet energy state ($^3E_{00}$) along with the oscillator strengths (*f*) are shown in the Table 2. The S_1 singlet state level of all the chlorins were determined experimentally from the intersection of the normalized absorption and emission spectra ($^1E_{00}$). The results of these theoretical calculations agree with the ones presented in the experimental section. This is exemplified by looking at the HOMO-1 of the metallochlorins (**Zn1** and **Zn2**). The HOMO-1 is lower in the Zn(II) compounds than the free base chlorins which undergo destabilization (**$H_2$1** and **$H_2$2**), displaying lower energy gaps [(HOMO-1) – LUMO] and [(HOMO-1) – (LUMO+1)].

Table 2. Molecular orbital energies (eV) and differences between HOMO/LUMO and singlet and triplet excited states from TDDFT calculations.

Chlorin	LUMO – HOMO	LUMO – (HOMO-1)	(LUMO+1) – (HOMO-1)	f [a]	$^1E_{00}$	$^3E_{00}$	ΔE_{S-T}	$^1E_{00}$ [b]
Zn1	2.554	2.89	3.548	0.1212	2.29	1.525	0.77	2.05
Zn2	2.548	2.94	3.608	0.1363	2.29	1.518	0.77	2.04
$H_2$1	2.632	2.76	3.295	0.0600	2.24	1.449	0.79	1.95
$H_2$2	2.631	2.79	3.338	0.0754	2.25	1.454	0.79	1.94

[a] Oscillator strength of transition $S_0 \rightarrow S_1$; [b] experimental value for S_1.

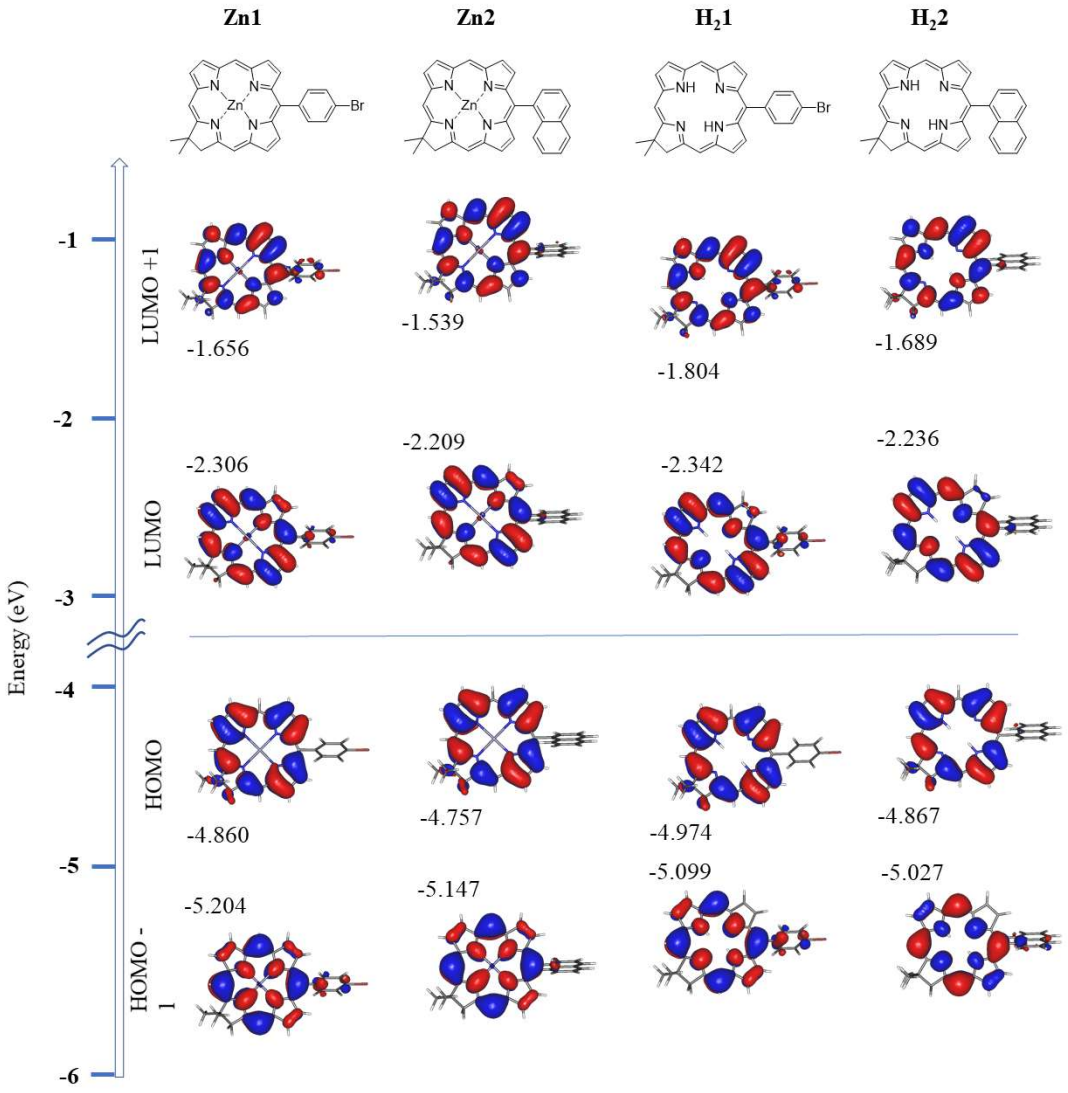

Figure 5. Molecular orbital energies and electron-density distribution obtained from DFT calculations.

X-ray Crystallography. Crystals suitable for single crystal X-ray diffraction analysis were grown by slow layer diffusion. For **Zn1**, the chlorin was dissolved in CH_2Cl_2, and layered with hexane. For **$H_2$1**, a CH_2Cl_2/hexane mixture evaporated slowly at rt. Crystals of poor quality were obtained with **Zn1** a CH_2Cl_2/hexane solvate and the **$H_2$1** poorly diffracting. The free base and metallated chlorins are shown in Figure 6 (see Table S2 for crystal data). The structure of **$H_2$1** is notably planar. Partial bromination of the C ring occurred during synthesis with approx. 3% present in the structure. Hydrogen atoms inside the chlorin were located. The Zn is displaced from the plane of the chlorin by ca. 0.315 Å. In both the **$H_2$1** and **Zn1** structures the phenyl ring is twisted to the chlorin plane (64.7° in **$H_2$1** and 63.03(19)° in **Zn1**). Further information and figures are given in the Supporting Information.

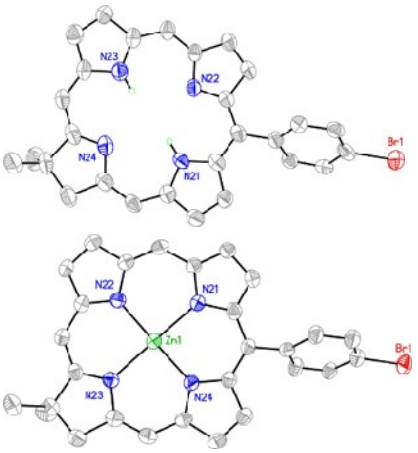

Figure. 6. View of the molecular structures of **$H_2$1** (top) and **Zn1** (bottom) in the crystal, shown with displacement at 50% probability and heteroatoms labelled. Inner chlorin hydrogen atoms shown in **$H_2$1**, all others omitted for clarity.

Conclusions

The synthesis, photophysical characterization and, singlet oxygen generation for chlorins **Zn1**, **Zn2** and their free base counterparts **$H_2$1**, **$H_2$2** was performed. Along with this, we have successfully obtained single crystal X-ray structures of **Zn1** and **$H_2$1**. Prior to this work, such complexes have not been investigated regarding their singlet oxygen generation and we have found that both **Zn1** and **Zn2** exhibit high triplet state yields (Φ_{isc} = 0.70 – 0.90) and excellent singlet oxygen quantum yields in methanol and ethanol (Φ_{Δ} = 0.60 – 0.85), in comparison the free base analogues exhibited suitable singlet oxygen quantum yields (Φ_{Δ} = 0.40 – 0.70). Results show that the chlorins are excellent PS candidates for PDT, given that they display high singlet oxygen quantum yields in polar solvents, modest fluorescence quantum yield and moderate triplet state lifetimes and yields upon photoexcitation.

Future work will include the optimization of the photophysical characteristics (red shifting the absorption bands, along with increasing the intensity of the Q_y absorption) through modification of the periphery with a variety of substituents, along with enhancement of the water-solubility for future *in vitro* evaluation.

Experimental Section

Synthesis

General information, instrumentation and crystallography. This is provided in the Supplementary Information.

1-Formyl-5-(4-bromophenyl)dipyrromethane (9a). The Vilsmeier reagent was prepared following a standard procedure.[31] DMF (11.5 mL, 151 mmol) was added to a dry round bottom flask and cooled to 0 °C, then $POCl_3$ (1.8 mL, 19.3 mmol) was added dropwise and stirred for 30 minutes under argon. To a separate dry round bottom flask **8a** (6.5 g, 21.5 mmol) was dissolved in DMF (20 mL) under argon and cooled to 0 °C. The Vilsmeier reagent was added dropwise to the reaction mixture and stirred at 0 °C for 2 h. A solution of EtOAc (100 mL) and sat. aq. NaOAc (100 mL) was added and stirred at room temperature for 3 h. The mixture was extracted with EtOAc (3 × 50 mL). The combined organic extracts were washed with brine (3 × 40 mL), $NaHCO_3$ (3 × 40 mL), water (3 × 40 mL), dried (Na_2SO_4) and concentrated to give a brown solid. The product was purified as the second fraction via column chromatography (SiO_2, hexane : EtOAc, 85:15, *v*/*v*) resulting in a light brown solid (2.745 g, 8.5 mmol, 39%); M.p.: dec. >150 °C; R_f = 0.57 (SiO_2, hexane:EtOAc, 3:2, *v*/*v*); ^{1}H NMR (400 MHz, $CDCl_3$): δ = 5.46 (s, 1 H, meso-*H*), 5.92 – 5.94 (m, 1 H, *β*-*H*), 6.05 – 6.06 (m, 1 H, *β*-*H*), 6.15 – 6.17 (q, *J* = 6.0, 2.7 Hz, 1 H, *β*-*H*), 6.72 – 6.74 (m, 1 H, *β*-*H*), 6.88 – 6.90 (m, 1 H, *β*-*H*), 7.04 – 7.06 (d, *J* = 8 Hz, 2 H, Ar-*H*), 7.43 – 7.45 (d, *J* = 8 Hz, 2 H, Ar-*H*), 7.98 (br s, 1 H, -N*H*), 9.17 (br s, 1 H, -N*H*), 9.37 ppm (s, 1 H, -C*H*O); ^{13}C NMR (101 MHz, $CDCl_3$): δ = 43.5, 108.1, 108.8, 110.8, 118.2, 121.4, 122.0, 129.7, 129.9, 131.9, 132.4, 139.4, 141.6, 178.7 ppm; DIP-MS *m/z* calcd. for $C_{16}H_{13}BrN_2O$ $[M]^+$: 329.1970, found: 329.0401.

1-Formyl-5-(1-naphthyl)dipyrromethane (9b). Following the same procedure as for **9a**. DMF (6 mL, 77.4 mmol) was added to a dry round bottom flask and cooled to 0 °C, then $POCl_3$ (0.9 mL, 7.2 mmol) was added dropwise and stirred for 30 min under argon. To a separate dry round bottom flask **8b** (3 g, 11 mmol) was dissolved in DMF (14 mL) and cooled to 0 °C. The Vilsmeier reagent was added dropwise to the reaction mixture and stirred at 0 °C for 1 h under argon. A solution of EtOAc (100 ml) and sat. aq. NaOAc (100 mL) was added and stirred at room temperature for 2 h. The mixture was extracted with EtOAc (3 × 50 mL). The combined organic phase was washed with brine (3 × 40 mL), $NaHCO_3$ (3 × 40 mL), water (3 × 40 mL), dried (Na_2SO_4) and concentrated to give a yellow oily product. The oil was adsorbed onto silica (CH_2Cl_2) and purified via column chromatography (SiO_2, hexane:EtOAc, 85:15, *v*/*v*). Elution of the second fraction (orange color) gave a beige solid (1.400 g, 4.6 mmol, 42%); M.p.: dec. >100 °C; R_f = 0.63 (SiO_2, hexane : EtOAc, 3:2, *v*/*v*); ^{1}H NMR (400 MHz, $CDCl_3$): δ = 5.99 (br, 1 H, *β*-*H*), 6.10 – 6.11 (m, 1 H, *β*-*H*), 6.17 – 6.19 (q, *J* = 2.7 Hz, 1 H, *β*-*H*), 6.28 (s, 1 H, meso-*H*), 6.69 – 6.70 (m, 1 H, *β*-*H*), 6.90 – 6.92 (m, 1 H, *β*-*H*), 7.10 – 7.12 (d, *J* = 7.1 Hz, 1 H, Ar-*H*), 7.39 – 7.42 (t, *J* = 7.6 Hz, 1 H, Ar-*H*), 7.43 – 7.50 (m, 2 H, Ar-*H*), 7.80 – 7.82 (d, *J* = 8.3 Hz, 1 H, Ar-*H*), 7.85 – 7.89 (m, 2 H, Ar-*H*, -N*H*), 7.94 – 7.96 (d, *J* = 9.2 Hz, 1 H, Ar-*H*), 9.00 (br s, 1 H, -N*H*), 9.39 ppm (s, 1 H, -C*H*O); ^{13}C NMR (101 MHz, $CDCl_3$): δ = 40.4, 108.2, 108.8, 110.9, 117.8, 121.9, 123.1, 125.5, 125.9, 126.2, 126.7, 128.5, 128.9, 129.9, 131.2, 132.2, 134.0, 136.1, 141.9, 178.5 ppm; DIP-MS *m/z* calcd. for $C_{20}H_{16}N_2O$ $[M]^+$: 300.1263, found: 300.1386.

9-Bromo-1-formyl-5-(4-bromophenyl)dipyrromethane (10a). Following a previously reported procedure,[32] to a dry Schlenk tube was added **9a** (400 mg, 1.2 mmol, 1 eq.), which was dried under high vacuum and dissolved in dry THF (10 mL) and the resulting solution was cooled to -78 °C, under argon. NBS (216 mg, 1.2 mmol, 1 eq.) was dissolved in anhydrous THF (5 mL), and then was added dropwise to **9a**. The reaction was left stirring under argon for 1 h. Hexane (30 mL) and water

(30 mL) were added and the cooling bath was removed. The mixture was allowed to warm to room temperature and then extracted with EtOAc (3 × 30 mL), dried (Na_2SO_4) and concentrated under low pressure to give a brown solid. **NOTE:** The water bath temperature should not exceed 25 °C. The product was purified via column chromatography (SiO_2, hexane:EtOAc, 85:15, *v/v*). The product eluted in the first fraction and was yielded as a light brown solid (350 mg, 0.85 mmol, 70%); M.p.: dec. >100 °C; R_f = 0.65 (SiO_2, hexane : EtOAc, 3:2, *v/v*); ^{1}H NMR (400 MHz, THF-d_8): δ = 5.44 (s, 1 H, meso-*H*), 5.63 – 5.64 (m, 1 H, *β*-*H*), 5.90 – 5.91 (m, 1 H, *β*-*H*), 5.97 – 5.98 (dd, *J* = 3.4, 2.4 Hz, 1 H, *β*-*H*), 6.83 – 6.85 (dd, *J* = 3.7, 2.4 Hz, 1 H, *β*-*H*), 7.13 – 7.16 (m, 2 H, Ar-*H*), 7.46 – 7.50 (m, 2 H, Ar-*H*), 9.44 (s, 1 H, -C*H*O), 10.55 (br s, 1 H, -N*H*), 11.26 ppm (br s, 1 H, -N*H*); ^{13}C NMR (101 MHz, THF-d_8): δ = 43.5, 97.2, 109.1, 109.3, 109.9, 120.4, 130.3, 131.2, 133.0, 133.5, 140.7, 141.2, 177.6 ppm; DIP-MS *m/z* calcd. for $C_{16}H_{12}Br_2N_2O$ $[M]^+$: 408.0930, found: 408.9592.

9-Bromo-1-formyl-5-(1-naphthyl)dipyrromethane (10b). Following the same procedure as for **9a**. To a dry Schlenk tube was added **9b** (1.050 g, 3.5 mmol, 1 eq) which was dried under high vacuum, and dissolved in dry THF (12 mL) and the resulting solution was cooled to -78 °C under argon. NBS (622 mg, 3.5 mmol, 1 eq.) was dissolved in THF (12 mL) and was added dropwise to **9b**. After 1 h, hexane (30 mL) and water (30 mL) were added and the cooling bath was removed. The mixture was allowed to warm to room temperature and extracted with EtOAc (3 × 40 mL), dried (Na_2SO_4) filtered and concentrated under reduced pressure to give a dark orange oil. **NOTE:** The water bath temperature should not exceed 25 °C. The oil was adsorbed onto silica (EtOAc) and purified via column chromatography (SiO_2, hexane:EtOAc, 4:1, *v/v*). The product eluted in the first fraction and was obtained as a light brown solid (730 mg, 1.92 mmol, 55%); M.p.: dec. >100 °C; R_f = 0.68 (SiO_2, hexane : EtOAc, 3 : 2, *v/v*); ^{1}H NMR (400 MHz, THF-d_8: δ = 5.54 – 5.56 (t, *J* = 3.0 Hz, 1 H, *β*-*H*), 5.79 – 5.8 (m, 1 H, *β*-*H*), 5.92 – 5.93 (t, *J* = 2.9 Hz, 1 H, *β*-*H*), 6.20 (s, 1 H, meso-*H*), 6.77 – 6.79 (m, 1 H, *β*-*H*), 7.08 – 7.09 (d, *J* = 7.1 Hz, 1 H, Ar-*H*), 7.38 – 7.42 (t, *J* = 7.7 Hz, 1 H, Ar-*H*), 7.42 – 7.44 (m, 2 H, Ar-*H*), 7.77 – 7.79 (d, *J* = 8.2 Hz, 1 H, Ar-*H*), 7.85 – 7.87 (m, 1 H, Ar-*H*), 8.01 – 8.03 (m, 1 H, Ar-*H*), 9.41 (s, 1 H, -C*H*O), 10.56 (br s, 1 H, -N*H*), 11.28 ppm (br s, 1 H, -N*H*); ^{13}C NMR (101 MHz, THF-d_8): δ = 41.1, 97.7, 110.2, 110.4, 111.5, 124.1, 126.0, 126.1, 126.7, 128.3, 129.3, 132.5, 134.1, 134.3, 134.8, 138.1, 142.4, 178.4 ppm; DIP-MS *m/z* calcd. for $C_{20}H_{15}BrN_2O$ $[M]^+$: 379.2570, found: 379.0666.

[17,18-Dihydro-18,18-dimethyl-10-(naphthalen-1-yl)porphyrinato]zinc(II) (Zn2). To a flask was added **7** (33.6 mg, 176.6 µmol), **10b** (57.8 mg, 152.4 µmol), and anhydrous CH_2Cl_2 (4 mL). In a separate flask, *p*-TsOH·H_2O (111 mg, 0.583 mmol) and anhydrous MeOH (1 mL) were added. The two solutions were mixed and stirred at 20 °C for 0.5 h whilst protected from light. 2,2,6,6-tetramethylpiperidine (0.16 mL, 0.948 mmol) was added and the solution concentrated. The resulting solid was suspended in anhydrous MeCN (20 mL). Further 2,2,6,6-tetramethylpiperidine (0.55 mL, 3.26 mmol) was added along with anhydrous zinc acetate (358 mg, 1.95 mmol) and silver triflate (100 mg, 0.390 mmol). The solution was then heated at 90 °C for 20 h whilst protected from light. Excess solvent was removed under reduced pressure, and the residue was purified via flash column chromatography (SiO_2, CH_2Cl_2:hexane, 1:1, *v/v*). The product eluted in the second fraction, which was blue in color. Excess solvent was removed under reduced pressure to yield the product as a dark green-blue solid (29.0 mg, 54.7 µmol, 36%). M.p.: >250 °C; R_f = 0.46 (SiO_2, CH_2Cl_2 : hexane, 1:1, *v/v*); ^{1}H NMR (400 MHz, $CDCl_3$): δ = 2.08 (s, 3 H, -CH_3), 2.09 (s, 3 H, -CH_3), 4.58 (s, 2 H, -CH_2-), 7.06 – 7.10 (m, 1 H, Ar-*H*), 7.19 – 7.21 (m, 1 H, Ar-*H*), 7.46 – 7.50 (m, 1 H, Ar-*H*), 7.82 – 7.86 (m, 1 H, Ar-*H*), 8.10 (d, *J* = 8 Hz, 1 H, Ar-*H*), 8.18 – 8.19 (m, 1 H, *β*-*H*), 8.20 – 8.28 (m, 2 H, Ar-*H*), 8.47 – 8.48 (d, *J* = 4.4 Hz, 1 H, *β*-*H*), 8.58 – 8.60 (d, 1 H, *J* = 4.4 Hz, *β*-*H*), 8.69 (s, 1 H, meso-*H*), 8.74 (s, 1 H, meso-*H*), 8.80 – 8.81 (d, *J* = 4.4 Hz, 1 H, *β*-*H*), 8.83 – 8.84 (d, *J* = 4.4 Hz, 1 H, *β*-*H*), 9.14 – 9.15 (d, *J* = 4 Hz, 1 H, *β*-*H*), 9.67 (s, 1 H, meso-*H*) ppm; ^{13}C NMR (101 MHz, $CDCl_3$): δ = 31.0, 45.3, 50.3, 94.4, 97.0, 109.5, 124.2, 125.5, 125.8, 127.0, 127.3, 127.8, 128.2, 128.4, 129.0, 131.5, 132.9, 132.9, 133.1, 136.3, 139.7, 146.0, 146.4, 147.9, 146.6, 153.2, 154.0, 159.4, 171.0 ppm; UV–Vis (EtOH): λ_{abs} (log ε) = 405 (5.54), 506 (3.73), 561 (3.83), 605 nm (4.76); HRMS calcd. for $C_{32}H_{24}N_4Zn$ [M+] 528.1292, found: 528.1301.

17,18-Dihydro-18,18-dimethyl-10-(naphthalen-1-yl)porphyrin ($H_2$2). To a round bottom flask was added **Zn2** (36.0 mg, 67.9 µmol) and CH_2Cl_2 (7 mL). To the resulting solution was added trifluoroacetic acid (0.20 mL, 2.62 mmol), and the mixture was stirred at 20 ºC for 1 h. TLC indicated the completion of the reaction and thus the reaction mixture was quenched with sat. $NaHCO_3$ soln. The layers were separated, and the organic phase was washed with sat. $NaHCO_3$ soln. (1 x 25 mL), water (1 x 25 mL), brine (1 x 25 mL) and dried ($MgSO_4$). The resulting solution was passed through a pad of silica (CH_2Cl_2) and excess solvent was removed under reduced pressure to yield the product as a dark green solid (13.0 mg, 27.9 µmol, 41%). M.p.: >300 °C, R_f = 0.66 (SiO_2, CH_2Cl_2:hexane, 1 : 1, *v/v*); ^{1}H NMR (600 MHz, $CDCl_3$): δ = - 2.19 (s, 1 H, N^{21}-*H*), -1.81 (s, 1 H, N^{23}-*H*), 2.09 (s, 3 H, -CH_3), 2.10 (s, 3 H, -CH_3), 4.66 (s, 2 H, -CH_2-), 7.08 – 7.10 (m, 1 H, Ar-*H*), 7.24 (d, *J* = 8.4 Hz, 1 H, Ar-*H*), 7.48 – 7.51 (m, 1 H, Ar-*H*), 7.84 – 7.87 (m, 1 H, Ar-*H*), 8.14 (d, *J* = 9 Hz, 1 H, Ar-*H*), 8.24 (d, *J* = 6.6 Hz, 1 H, Ar-*H*), 8.27 (d, *J* = 8.4 Hz, 1 H, Ar-*H*), 8.38 (d, *J* = 4.2 Hz, 1 H, *β*-*H*), 8.58 (d, *J* = 4.8 Hz, 1 H, *β*-*H*), 8.75 (d, *J* = 4.8 Hz, 1 H, *β*-*H*), 8.89 (d, *J* = 4.2 Hz, 1 H, *β*-*H*), 8.96 (s, 1 H, meso-*H*), 8.98 (d, *J* = 4.2 Hz, 1 H, *β*-*H*), 9.03 (s, 1 H, meso-*H*), 9.25 (d, *J* = 4.2 Hz, 1 H, *β*-*H*), 9.87 (s, 1 H, meso-*H*) ppm. ^{13}C NMR (151 MHz, $CDCl_3$): δ = 31.3, 31.3, 46.6, 52.2, 94.6, 97.0, 107.4, 107.4, 118.9, 123.3, 123.8, 124.4, 125.8, 126.1, 128.0, 128.3, 128.4, 128.5, 128.6, 132.1, 132.2, 132.7, 133.1, 134.4, 136.0, 136.6, 139.1, 139.7, 140.9, 151.1, 153.5, 163.2, 175.3 ppm. ^{15}N/^{1}H-HSQC ($CDCl_3$): 134.5 (N^{21}), 133.5 (N^{23}) ppm; UV–Vis (CH_2Cl_2): λ_{abs} (log ε) = 394 (5.15), 407 (5.24), 494 (4.11), 501 (4.17), 587 (3.70), 639 nm (4.64); HRMS *m/z* Calcd. for $[M+H^+]$ 467.2230, found: 467.2235 $[C_{32}H_{27}N_4+H^+]$.

5′ -[4-{(17,18-Dihydro-18,18-dimethylporphyrinato]zinc(II)-10-yl)phenyl-10′ , 20′ -diphenyl}porphyrinato] zinc(II) (12). Following literature procedures,[38] **Zn1** (96 mg, 171 µmol), [5,15-diphenyl-10,20-bis(4′,4′,5′,5′-tetramethyl-1′,3′,2′-dioxaborolan-2′-yl)porphinato]zinc(II)] **11** (100 mg, 129 µmol) and Cs_2CO_3 (280 mg, 857 µmol) were added in a dry Schlenk tube and left to dry *in vacuo* for 30 min. Then dry toluene/DMF (12 mL, 2:1) were added and the solution was degassed with argon for 20 min. $Pd(PPh_3)_4$ (20 mg, 17 µmol) was added and degassed with argon for 15 min. The reaction mixture was covered with foil and left stirring for 3 h at 85 °C. CH_2Cl_2 was added and the mixture was washed with $NaHCO_3$ (3 × 50 mL), brine (3 × 50 mL) and H_2O (3 × 50 mL). Dried over Na_2SO_4, filtered and evaporated under reduced pressure to give a dark purple solid. The product was purified by silica gel column chromatography or preparative TLC and recrystallized with Cl_2CH_2/hexane. Purification yielded a dark purple solid (17 mg, 17 µmol, 13%). M.p.: >250 °C; R_f = 0.64 (SiO_2, CH_2Cl_2); ^{1}H NMR (600 MHz, $CDCl_3$): δ = 2.11 (s, 6 H, C(CH_3)$_2$), 4.63 (s, 2 H, -CH_2-), 7.86 – 7.87 (m, 6 H, Ar-*H*), 8.35 – 8.36 (m, 4 H, Ar-*H*), 8.49 – 8.50 (d, *J* = 7.4 Hz, 2 H, Ar-H_{linker}), 8.59 – 8.60 (d, *J* = 7.5 Hz, 2 H, Ar-H_{linker}), 8.71 (s, 1 H, meso-*H*), 8.85 (s, 1 H, meso-*H*), 8.86 (m, 2 H, *β*-*H*), 9.01 (d, *J* = 4.0 Hz, 1 H, *β*-*H*), 9.07 – 9.08 (d, *J* = 4.0 Hz, 1 H, *β*-*H*), 9.19 (m, 4 H, *β*-*H*), 9.22 (m, 2 H, *β*-*H*), 9.45 – 9.47 (m, 4 H, *β*-*H*), 9.76 (s, 1 H, meso-*H*), 10.33 ppm (s, 1 H, meso-*H*); ^{13}C NMR (151 MHz, $CDCl_3$): δ = 31.0, 45.45, 50.4, 94.4, 97.2, 106.0, 106.1, 109.6, 120.8, 120.8, 121.5, 123.5, 126.6, 127.0, 127.5, 127.6, 128.4, 129.3, 131.8, 131.8, 132.1, 132.1, 132.2, 132.2, 132.7, 132.8, 133.1, 133.3, 134.6, 141.7, 142.0, 142.7, 146.1, 146.1, 146.7, 147.5, 150.0, 150.1, 150.3, 150.3, 150.3, 153.3, 154.2, 159.4, 171.2 ppm; UV–Vis (CH_2Cl_2): λ_{max} (log ε) = 403 (4.89), 4.18 (5.40), 544 (3.87), 607 nm (4.06); HRMS (MALDI) *m/z* calcd. for $C_{60}H_{40}N_8Zn_2$ $[M]^+$: 1000.1959, found: 1000.1971.

Acknowledgments

This work has received funding from the European Union's Horizon 2020 research and innovation programme under the

Marie Skłodowska-Curie Grant Agreement No. 764837 and was supported by a grant from Science Foundation Ireland (IvP 13/IA/1894). We thank Dr. Nitika Grover for her invaluable assistance throughout this project and providing compound **11**.

Keywords: • dihydroporphyrin • chlorin • photodynamic therapy • singlet oxygen • triplet yields • photophysical characterization

References

[1] M. G. H. Vicente, *Curr. Med. Chem.: Anti-Cancer Agents* **2001**, *1*, 175–194.

[2] R. Bonnett, P. Charlesworth, B. D. Djelal, D. J. McGarvey, T. G. Truscott, *J. Chem. Soc., Perkin Trans. 2* **1999**, *2*, 325–328.

[3] Y. Chen, G. Li, R. K. Pandey, *Curr. Org. Chem.* **2004**, *8*, 1105–1134.

[4] D. Lafont, Y. Zorlu, H. Savoie, F. Albrieux, V. Ahsen, R. W. Boyle, F. Dumoulin, *Photodiagn. Photodyn. Ther.* **2013**, *10*, 252–259.

[5] a) Z. Wu, T. Wang, Y. Meng, Y. Rao, B. Wang, J. Zheng, S. Gao J. Zhang, *Chem. Sci.* **2017**, *8*, 5953 – 5961; b) A. G. Maher, G. Passard, D. K. Dogutan, R. L. Halbach, B. L. Anderson, C. J. Gagliardi, M. Taniguchi, J. S. Lindsey, D. G. Nocera, *ACS Catal.* **2017**, *7*, 3597 – 3606; c) X. Wang, H. Tamiaki, L. Wang, N. Tamai, O. Kiato, H. Zhou, S. Sasaki, *Langmuir*, **2010**, *26*, 6320 – 6327; d) Y, Li, Y. Feng, Y. Wang, C. Fan, X. Liu, X. Li, B. Zheng, *Int. J. Quantum Chem.* **2014**, *114*, 222 – 232; e) K. Mase, K. Ohkubo, S. Fukuzumi, *J. Am. Chem. Soc.* **2013**, *135*, 2800 – 2808.

[6] M. O. Senge, A. A. Ryan, K. A. Letchford, S. A. MacGowan, T. Mielke, *Symmetry* **2014**, *6*, 781–843.

[7] a) M. Gouterman, *J. Mol. Spectrosc.* **1961**, *6*, 138–163; b) M. Gouterman, G. H. Wagnière, L. C. Snyder, *J. Mol. Spectrosc.* **1963**, *11*, 108–127; c) P. J. Spellane, M. Gouterman, A. Antipas, S. Kim, Y. C. Liu, *Inorg. Chem.* **1980**, *19*, 386–391.

[8] K. E. Borbas, V. Chandrashaker, C. Muthiah, H. L. Kee, D. Holten, J. S. Lindsey, *J. Org. Chem.* **2008**, *73*, 3145–3158.

[9] E. F. F. Silva, F. A. Schaberle, C. J. P. Monteiro, J. M. Dąbrowski, L. G. Arnaut, *Photochem. Photobiol. Sci.* **2013**, *12*, 1187–1192.

[10] E. G. Azenha, A. C. Serra, M. Pineiro, M. M. Pereira, J. Seixas de Melo, L. G. Arnaut, S. J. Formosinho, A. M. d. A. R. Gonsalves, *Chem. Phys.* **2002**, *280*, 177–190.

[11] J. Zhao, W. Wu, J. Sun, S. Guo, *Chem. Soc. Rev.* **2013**, *42*, 5323–5351.

[12] D. Kilin, U. Kleinekathöfer, M. Schreiber, *J. Phys. Chem. A.* **2000**, *104*, 5413–5421.

[13] a) F. Li, S. Gentemann, W. A. Kalsbeck, J. Seth, J. S. Lindsey, D. Holten, D. F. Bocian, *J. Mat. Chem.* **1997**, *7*, 1245–1262; b) N. M. Barbosa Neto, D. S. Correa, L. De Boni, G. G. Parra, L. Misoguti, C. R. Mendonça, I. E. Borissevitch, S. C. Zílio, P. J. Gonçalves, *Chem. Phys. Lett.* **2013**, *587*, 118–123; c) L. Ye, *Sci. Bull.* **2008**, *53*, 3615–3619.

[14] M. Bregnhoj, M. Westberg, F. Jensen, P. R. Ogilby, *Phys. Chem. Chem. Phys.* **2016**, *18*, 22946–22961.

[15] a) A. P. Castanoa, T. N. Demidovaa, M. R. Hamblin, *Photodiagn. Photodyn. Ther.* **2004,** *1*, 279–293; b) H. Abrahamse, M. R. Hamblin, *Biochem. J.* **2016**, *473*, 347–364.

[16] a) R. R. Allison, G. H. Downie, R. Cuenca, X. H. Hu, C. J. H. Childs, C. H. Sibata, *Photodiagn. Photodyn. Ther.* **2004**, *1*, 27–42. b) J. M. Dąbrowski, L. G. Arnaut, *Photochem. Photobiol. Sci.* **2015**, *14*, 1765–1780.

[17] E. F. Gudgin, J. C. Kennedy, R. H. Pottier, in Photodynamic Therapy, ed. T. Patrice, Royal Society of Chemistry, Cambridge, 1st edn., 2003, ch. 3, pp. 81 – 104.

[18] V. H. Fingar, P. K. Kik, P. S. Haydon, P. B. Cerrito, M. Tseng, E. Abang, T. J. Wieman, *Br. J. Cancer* **1999**, *79*, 1702 – 1708.

[19] A. Juzeniene, *Photodiagn. Photodyn. Ther.* **2009**, *6*, 94 – 96.

[20] J. Son, G. Yi, M-H. Kwak, S. M. Yang, J. M. Park, B-I. Lee, M-G. Choi, H. Koo, *J. Nanonbiotechnol.* **2019**, *17*, 50.

[21] K. J. Lorenz, H. Maeir, *HNO*, **2008**, *56*, 402 – 409.

[22] M. O. Senge, *Photodiagn. Photodyn. Ther.*, **2012**, *9*, 170 – 179.

[23] M. K. Kuimova, G. Yahioglu, P. R. Ogilby, *J. Am. Chem. Soc.* **2009**, *131*, 332 – 340.

[24] J. S. Lindsey, *Chem. Rev.* **2015**, *115*, 6534 – 6620.

[25] C. J. Dutton, C. J. R. Fookes, A. R. Battersby, *J. Chem. Soc., Chem. Commun.* **1983**, *21*, 1237 – 1238.

[26] J. -P. Strachan, D. F. O'Shea, T. Balasubramanian, J. S. Lindsey, *J. Org. Chem.* **2000**, *65*, 3160 – 3172.

[27] M. Taniguchi, D. Ra, G. Mo, T. Balasubramanian, J. S. Lindsey, *J. Org. Chem.* **2001**, *66*, 7342 – 7354.

[28] M. Ptaszek, J. Bhaumik, H. -J. Kim, M. Taniguchi, J. S. Lindsey, *Org. Process Res. Dev.* **2005**, *9*, 651 – 659.

[29] M. Krayer, M. Ptaszek, H.-J. Kim, K. R. Meneely, D. Fan, K. Secor, J. S. Lindsey, *J. Org. Chem.* **2010**, *75*, 1016 – 1039.

[30] a) C. H. Lee, J. S. Lindsey, *Tetrahedron* **1994**, *50*, 11427–11440; b) B. J. Littler, M. A. Miller, C. H. Hung, R. W. Wagner, D. F. O'Shea, P. D. Boyle, J. S. Lindsey, *J. Org. Chem.* **1999**, *64*, 1391–1396; c) J. K. Laha, S. Dhanalekshmi, M. Taniguchi, A. Ambroise, J. S. Lindsey, *Org. Process Res. Dev.* **2003**, *7*, 799–812.

[31] M. Ptaszek, B. E. McDowell, J. S. Lindsey, *J. Org. Chem.* **2006**, *71*, 4328–4331.

[32] a) O. Mass, M. Ptaszek, M. Taniguchi, J. R. Diers, H. L. Kee, D. F. Bocian, D. Holten, J. S. Lindsey, *J. Org. Chem.* **2009**, *74*, 5276–5289; b) J. K. Laha, C. Muthiah, M. Taniguchi, B. E. McDowell, M. Ptaszek, J. S. Lindsey, *J. Org. Chem.* **2006**, *71*, 4092–4102.

[33] M. Ptaszek, B. E. McDowell, M. Taniguchi, H.J. Kim, J. S. Lindsey, *Tetrahedron* **2007**, *63*, 3826–3839.

[34] A. I. Arkhypchuk, R. Xiong, K. Eszter Borbas, *J. Inorg. Biochem.* **2020**, *205*, 110979.

[35] C. Muthiah, D. Lahaye, M. Taniguchi, M. Ptaszek, J. S. Lindsey, *J. Org. Chem.* **2009**, *74*, 3237–3247.

[36] N. Miyaura, A. Suzuki, *Chem. Rev.* **1995**, *7*, 2457 – 2483.

[37] K. Sonogashira, *J. Organomet. Chem. 2002*, **653**, *1*, 46 – 49.

[38] a) R. W. Wagner, Y. Ciringh, C. Clausen, J. S. Lindsey, *Chem. Mater.* **1999**, *11*, 2974-2983; b) M. Taniguchi, M. N. Kim, D. Ra, J. S. Lindsey, *J. Org. Chem.* **2005**, *70*, 275–285; c) M. O. Senge, Y. M. Shaker, M. Pintea, C. Ryppa, S. S. Hatscher, A. Ryan, Y. Sergeeva, *Eur. J. Org. Chem.* **2010**, 2237–2258.

[39] A. G. Hyslop, M. A. Kellett, P. M. Iovine, M. J. Therien, *J. Am. Chem. Soc.* **1998**, *120*, 12676−12677.

[40] a) K. S. Kim, J. M. Lim, A. Osuka, D. Kim, *J. Photochem. Photobiol. C* **2008**, *9*, 13–28; b) L. M. Mazur, T. Roland, S. Leroy-Lhez, V. Sol, M. Samoc, I. D. W. Samuel, K. Matczyszyn, *J. Phys. Chem. B*, **2019**, *123*, 4271–4277.

[41] a) R. Giovannetti, *Macro to Nano Spectrosc.* **2012**, *1*, 87–108; b) D. Marsh, L. Mink, *J. Chem. Educ.* **1996**, *73*, 1188–1190.

[42] a) M. Gouterman, in The Porphyrins, D. Dolphin ed., Academic Press, New York **1978**, *3*, 1–165; b) K. Aravindu, H.-J. Kim, M. Taniguchi, P. L. Dilbeck, J. R. Diers, D. F. Bocian, D. Holten, J. S. Lindsey, *Photochem. Photobiol. Sci.* **2013**, *12*, 2089−2109.

[43] N. Chaudhri, N. Grover, M. Sankar, *Inorg. Chem.* **2017**, *56*, 11532−11545.

[44] a) S. Gentemann, C. J. Medforth, T. P. Forsyth, D. J. Nurco, K. M. Smith, J. Fajer, D. J. Holten, *J. Am. Chem. Soc.* **1994**, *116*, 7363−7368; b) A. K. Mandal, T. Sahin, M. Liu, J. S. Lindsey, D. F. Bocian, D. Holten, *New J. Chem.* **2016**, *40*, 9648–9656; c) M. Liu, C. Y. Chen, A. K. Mandal, V. Chandrashaker, R. B. Evans-Storms, J. B. Pitner, D. F. Bocian, D. Holten, J. S. Lindsey, *New J. Chem.* **2016**, *40*, 7721–7740.

[45] R. Liu, M. Liu, D. Hood, C. Y. Chen, C.J. MacNevin, D. Holten, J.S. Lindsey, *Molecules* **2018**, *23*, 130.

[46] a) F. Wilkinson, A. A. Abdel-Shafi, *J. Phys. Chem. A* **1997,** *101*, 5509–5516; b) A. Beeby, A. E. Jones, *Photochem. Photobiol.* **2000**, *72*, 10–15.

[47] S. L. Murov, I. Carmicael, G. L. Hug, Handbook of Photochemistry, Markel Dekker, New York, 2nd ed. **1993**.

[48] A. Bautista-Sanchez, A. Kasselouri, M. C. Desroches, J. Blais, P. Maillard, D. M. de Oliveira, A. C. Tedesco, P. Prognon, J. Delaire, *J. Photochem. Photobiol. B: Biol.* **2005**, *81*, 154–162.

[49] J. M. Dąbrowski, L. G. Arnaut, M. M. Pereira, K. Urbańska, S. Simões, G, Stochel, L. Cortes, *Free Radic. Biol. Med.* **2012**, *52*, 1188–1200.

[50] a) M. A. Filatov, S. Karuthedath, P. M. Polestshuk, H. Savoie, K. J. Flanagan, C. Sy, E. Sitte, M. Telitchko, F. Laquai, R. W. Boyle, M. O.

Senge, *J. Am. Chem. Soc.* **2017**, *139*, 6282–6285; b) X. F. Zhang, X. Li, *J. Lumin.* **2011**, *131*, 2263–2266.

[51] F. Wilkinson, W. P. Helman, A. B. Ross, *J. Phys. Chem. Ref. Data* **1995**, *24*, 663–677.

[52] H. K. Kee, C. Kirmaier, Q. Tang, J. R. Diers, C. Muthiah, M. Taniguchi, J. K. Laha, M. Ptaszek, J. S. Lindsey, D. F. Bocian, D. Holten, *Photochem. Photobiol.* **2007**, *83*, 1125–1143.

[53] C. Brückner, J. R. McCarthy, H. W. Daniell, Z. D. Pendon, R. P. Ilagan, T. M. Francis, L. Ren, R. R. Birge, H. A. Frank, *Chem. Phys.* **2003**, *294*, 285–303.

Entry for the Table of Contents (Please choose one layout)

Layout 2:

FULL PAPER

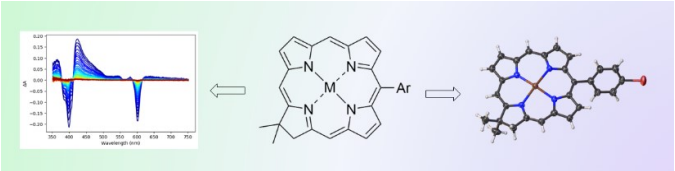

We present the synthesis of 17,18-dihydro-18,18-dimethylporphyrins bearing different substituents at the meso-position along with their photophysical characterization, DFT calculations and, in two cases, single crystal X-ray structures. Their photophysical properties are envisaged to be optimized through peripheral and conformational modulation with maintaining the singlet oxygen generation.

Chlorins, Photophysics*

Zoi Melissari,[a,b] Harry C. Sample,[a] Brendan Twamley,[c] René M. Williams[b] and Mathias O. Senge*[a]*

Page No. – Page No.

Synthesis and spectral properties of *gem*-dimethyl chlorin photosensitizers